第 49 卷第 2 期
七月 2025

Diqiu Kexue - Zhongguo Dizhi Daxue Xuebao/Earth Science
Journal of China University of Geosciences

Vol. 50 No. 2
July - Dec 2025

DOI: 10.5281/zenodo.17934732

Finite Element Evaluation of Frames with Concrete-Confined Steel Composite Columns: Effects of Concrete Strength and Steel Yield Stress

Moein Shirdel *

School of Civil Engineering, Iran University of Science and Technology (IUST), Tehran, Iran

*Corresponding author: moein_shirdel@cmps2.iust.ac.ir

Published: 15 December 2025
Accepted: 19 November 2025
Received: 08 October 2025

Abstract: This study investigates the structural response of frames incorporating concrete-confined steel composite columns through a nonlinear three-dimensional finite element analysis. The inelastic behavior of concrete, steel sections, longitudinal and transverse reinforcements, as well as the confinement effects provided by concrete encasement, are modeled using ABAQUS. Three frame configurations—featuring SRC beams, steel section beams, and reinforced concrete beams—are analyzed to evaluate the influence of concrete compressive strength and steel yield stress on global frame behavior and load-carrying capacity. The numerical results reveal that increasing both concrete strength and steel yield stress enhances frame performance and strength. The strengthening effect of concrete compressive strength is more significant in frames with SRC beams, while the improvement due to higher steel yield stress is more pronounced in frames with steel beams. For frames equipped with reinforced concrete beams, both parameters contribute almost equally to the enhancement of structural behavior.

Keywords: *Composite Column, Frame, Nonlinear Analysis, Confinement*

1. Introduction

Composite steel–concrete columns have gained substantial attention in recent decades due to their superior mechanical performance, efficient load-carrying capacity, and enhanced ductility compared with conventional reinforced concrete (RC) and steel columns. The interaction between the encased steel section and surrounding concrete leads to significant confinement effects, which in turn improve the compressive strength, stiffness, and energy absorption capacity of the structural members. These advantages have contributed to the increasing application of steel-reinforced concrete (SRC) and concrete-encased steel composite columns in mid-rise and high-rise structures, especially in seismic regions (Han et al., 2020; Tao et al., 2018). Previous studies have demonstrated that composite columns exhibit enhanced stability and reduced susceptibility to local buckling when adequately confined (Uy et al., 2011). Additionally, the confinement provided by concrete encasement delays steel yielding and improves post-peak behavior under both monotonic and cyclic loading (Zheng et al., 2017). Such benefits have motivated researchers to further investigate the nonlinear response of composite members and frames using advanced numerical modeling techniques.

Advancements in finite element (FE) methods have made it possible to accurately simulate the interaction between steel sections, concrete, and reinforcement under complex loading scenarios. Studies employing ABAQUS and similar FE platforms have shown strong agreement with experimental data for SRC composite columns and beam-column joints (Li et al., 2019; Hossain & Ahmed, 2021). These numerical tools enable the investigation of parameters that are difficult or costly to evaluate experimentally, such as confinement intensity, steel yield stress, and concrete compressive strength. A significant body of recent research has focused on the influence of material properties on the global behavior of SRC frames. For instance, (Wang et al,2021) highlighted that increases in concrete strength substantially enhance load-carrying capacity and stiffness, while (Zhang et al, 2022) demonstrated that steel yield strength plays a crucial role in improving ductility and delaying local buckling in composite sections. Despite these efforts, comparative studies examining different beam types within SRC column-based frames—such as steel beams, RC beams, and SRC beams—remain limited.

Given the wide use of composite systems in practical construction and the need to optimize structural performance, a more detailed numerical assessment is required to understand how variations in concrete compressive strength and steel yield stress influence the behavior of frames incorporating concrete-confined steel composite columns. This study aims to address this gap by conducting a comprehensive nonlinear 3D finite element analysis of multiple frame configurations using ABAQUS. The findings are expected to provide important insights that can support improved design strategies and performance-based engineering approaches for modern steel–concrete composite structures.

2. Method and Materials

The concrete-confined steel composite column used in this study consists of four components: the steel section, longitudinal reinforcement, transverse reinforcement, and the surrounding concrete (Fig. 1). Earlier studies on reinforced concrete columns, such as those by (Mirza,1989), indicate that the concrete region can be divided into an effectively confined core and an outer unconfined zone that includes the cover concrete and the parabolic region between longitudinal bars. In composite columns with concrete encasement, confinement is provided by both the steel section and the reinforcement cage. The level of confinement is influenced by several factors, including steel-section geometry, reinforcement size and spacing, and material properties such as steel yield strength and concrete compressive strength. Increased confinement pressure enhances both the strength and ductility of concrete. Based on these mechanisms, the concrete can be classified into three regions:

(1) unconfined concrete, located outside the parabolic boundary of reinforcement;

(2) highly confined concrete, located within the steel-section boundaries; and

(3) partially confined concrete, positioned between the confined core and the outer unconfined region.

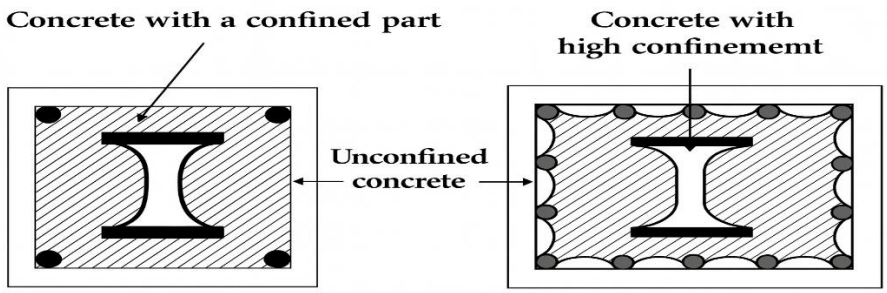

Fig 1. *Confinement area in concrete-confined steel composite column.*

Analytical studies by Chen and Lin (2006) showed that confinement levels vary with steel-section form and reinforcement layout. Mirza and Skrabek (1992) further demonstrated that the parabolic confinement boundaries may be idealized as rectangular regions, where the highly confined zone extends from the steel web to half the flange width, the partially confined region extends to the centroid of longitudinal reinforcement, and the remaining outer area is considered unconfined.

Concrete

For the 3D modeling of concrete, 8-node reduced-integration solid elements (C3D8R) were used due to their numerical efficiency and reliable convergence in nonlinear analysis. The Concrete Damaged Plasticity (CDP) model was adopted to simulate the nonlinear behavior of concrete, as validated in recent studies (Lee & Fenves, 2021; Yu & Teng, 2019). Concrete confinement is mainly provided by transverse reinforcement, which increases the strength and ductility of the concrete core. The confinement level is also influenced by longitudinal reinforcement arrangement, bar spacing, and loading type (Tao et al., 2018).

The constitutive stress–strain behavior of confined and unconfined concrete was modeled using an updated form of the Mander-type model, which remains widely supported in modern research (Niu et al., 2020; Zhang et al., 2022). The confined concrete stress–strain curve is given by:

The confined concrete stress–strain relationship is defined as:

$$f_c = (f'_{cc} * x) / (r - 1 + x^r) \quad (1)$$

$$x = \varepsilon_c / \varepsilon_{cc} \quad (2)$$

$$r = E_c / (E_c - E_{sec}) \quad (3)$$

Where:

f′cc is the compressive strength of confined concrete;

εcc is the maximum strain of confined concrete;

Ec is the tangent modulus;

Esec is the secant modulus at maximum stress:

$$E_{sec} = f'_{cc} / \varepsilon_{cc} \quad (4)$$

Maximum confined strain:

$$\varepsilon_{cc} = \varepsilon_{co}[1 + 5(f'_{cc}/f'_{co} - 1)] \quad (5)$$

Confined concrete strength:

$$f'_{cc} = f'_{co}(-1.254 + 2.254\sqrt{(1 + 7.94\, f'_l/f'_{co} - 2\, f'_l/f'_{co})}) \quad (6)$$

The confined concrete strength considering lateral pressure f'l is defined as:

$$f'cc = f'co * (-1.254 + 2.254 * \text{sqrt}(1 + 7.94(f'l / f'co) - 2(f'l / f'co)))$$

For unconfined concrete, f'l = 0 and εco = 0.002. The initial elastic modulus was estimated using the updated ACI expression:

$$Ec = 4700 * \text{sqrt}(f'c)$$

A Poisson's ratio of 0.2 was assumed in all models.

Boundary and Loading Conditions

For modeling loading sheets, discrete rigid 4-node 3D elements (R3D4) are used. The loading sheets are tied in the both ends of the column. In this study the ends of both SRC columns are enclosed corresponding to three directions of X, Y, and Z and also bind in a circle corresponding to three direction. On the top of the columns and beam there is no possibility of displacement in Y and Z directions and only the applied load would be as 50 mm displacement along the x axis parallel with the beam.

Frame Modeling and Parametric Study

All structural components were modeled in a three-dimensional space as deformable bodies, and a general static analysis procedure was adopted. The connections between the frame members were defined as described in the previous sections. Both material nonlinearity and geometric nonlinearity were considered in all analyses. Three frame configurations were modeled in this study. In all cases, the columns consisted of concrete-confined steel composite sections with dimensions of 160 × 160 mm and a height of 1000 mm, while the beam length was 1000 mm (Fig. 2). Frame 1 employed an SRC beam with the properties listed in Table 1. Frame 2 incorporated a steel-section beam with specifications shown in Table 2. Frame 3 utilized a reinforced concrete beam as detailed in Table 3.

The parametric study focused on evaluating the effects of concrete compressive strength and steel yield stress on the structural response under monotonic lateral loading. For each frame configuration, two levels of concrete compressive strength were considered (fc = 30 and 70 MPa), along with two yield stress values for the steel section (fys = 360 and 690 MPa). The reinforcement yield strength (fyr) was taken as 400 MPa. The stirrup spacing was set to 125 mm in the columns and 100 mm in the beams. Each section contained four longitudinal reinforcement bars of 4 mm diameter and transverse reinforcement of 6 mm diameter.

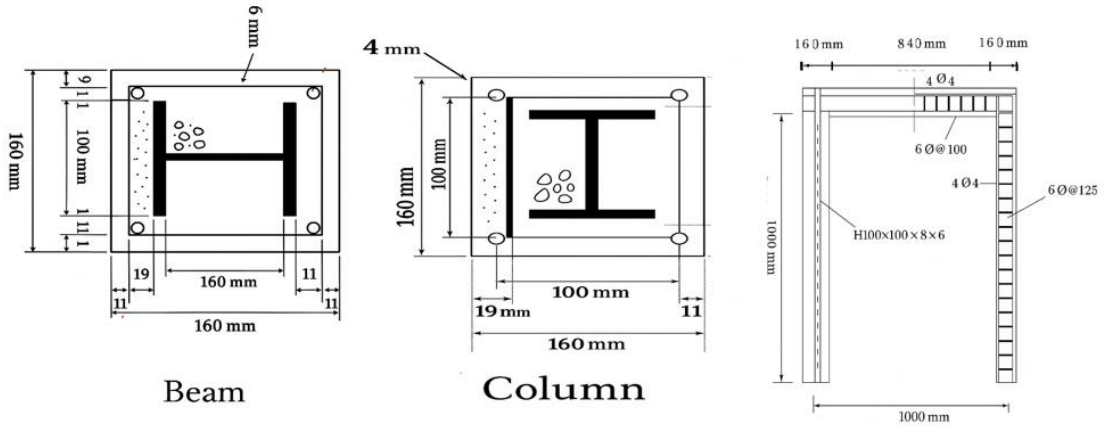

Fig 2. *Specifications of beam, columns, and frame sections*

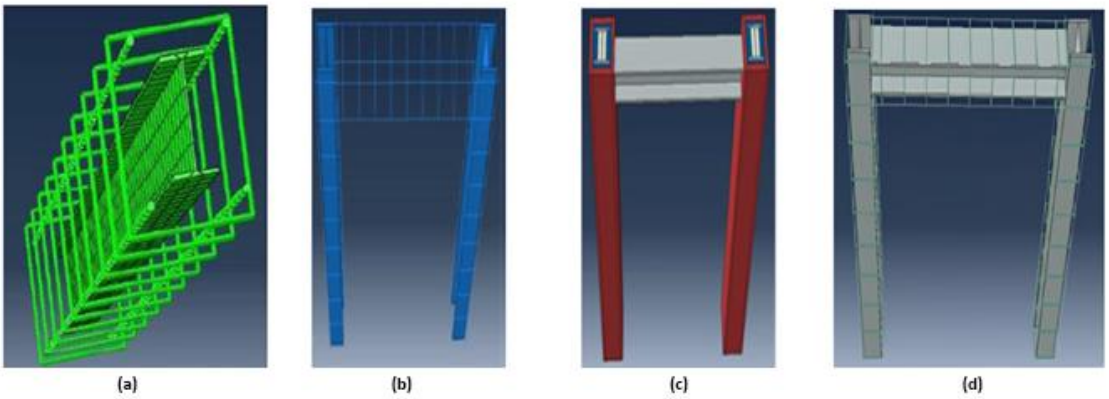

Fig 3. *Modeled frames. a) Finite element model of steel section with reinforcements, b) Frame with reinforced concrete beam, c) Frame with steel beam, d) Frame with concrete-confined steel composit beam*

Table 1. Specifications of dimensions and masonry of frame with SRC beam.

.

Sample	Member	Height (mm)	Steel Profile (mm)	Fc (MPa)	Fys (MPa)	Fyr (MPa)	Long. reinf. No	Long. reinf. Ø	Trans. reinf. S (mm)
Frame 1	Column	1000	H100×100×8×6	30	240	400	4	4	125
Frame 1	Beam	1000	H100×100×8×6	30	240	400	4	4	100
Frame 2	Column	1000	H100×100×8×6	70	240	400	4	4	125
Frame 2	Beam	1000	H100×100×8×6	70	240	400	4	4	100
Frame 3	Column	1000	H100×100×8×6	30	690	400	4	4	125
Frame 3	Beam	1000	H100×100×8×6	30	690	400	4	4	100
Frame 4	Column	1000	H100×100×8×6	70	690	400	4	4	125
Frame 4	Beam	1000	H100×100×8×6	70	690	400	4	4	100

Table 2. *Specifications of dimensions and masonry of frame with steel beam.*

Sample	Member	Height (mm)	Steel Profile (mm)	Fc (MPa)	Fys (MPa)	Fyr (MPa)	Long. reinf. No	Long. reinf. Ø	Trans. reinf. S (mm)
Frame 5	Column	1000	H100×100×8×6	30	240	400	4	4	125
Frame 5	Beam	1000	H100×100×8×6	30	240	400	4	4	100
Frame 6	Column	1000	H100×100×8×6	70	240	400	4	4	125
Frame 6	Beam	1000	H100×100×8×6	70	240	400	4	4	100
Frame 7	Column	1000	H100×100×8×6	30	690	400	4	4	125
Frame 7	Beam	1000	H100×100×8×6	30	690	400	4	4	100
Frame 8	Column	1000	H100×100×8×6	70	690	400	4	4	125
Frame 8	Beam	1000	H100×100×8×6	70	690	400	4	4	100

Table 3. *Specifications of dimensions and masonry of frame with reinforcement concrete beam.*

Sample	Member	Height (mm)	Steel Profile (mm)	Fc (MPa)	Fys (MPa)	Fyr (MPa)	Long. reinf. No	Long. reinf. Ø	Trans. reinf. S (mm)
Frame 9	Column	1000	H100×100×8×6	30	240	400	4	4	125
Frame 9	Beam	1000	H100×100×8×6	30	240	400	-	-	-
Frame 10	Column	1000	H100×100×8×6	70	240	400	4	4	125
Frame 10	Beam	1000	H100×100×8×6	70	240	400	-	-	-
Frame 11	Column	1000	H100×100×8×6	30	690	400	4	4	125
Frame 11	Beam	1000	H100×100×8×6	30	690	400	-	-	-
Frame 12	Column	1000	H100×100×8×6	70	690	400	4	4	125
Frame 12	Beam	1000	H100×100×8×6	70	690	400	-	-	-

3. Findings

Based on the results in Table 4, increasing both the concrete compressive strength and the steel section yield stress leads to an improvement in the overall frame strength. However, the influence of concrete compressive strength on enhancing the frame capacity is greater than that of increasing the steel section yield stress. Furthermore, the effect of increasing concrete strength is more pronounced in frames with a steel yield stress of 240 MPa compared to those with a yield stress of 690 MPa.

Table 4. *Results of FEA of frame with SRC beam.*

Sample	Py (kN)	Δy (mm)	Δu (mm)	μ
Frame 1	121.78	7	36.2	5.17
Frame 2	188.5	7.25	33.6	4.63
Frame 3	176.13	12.2	48.9	4
Frame 4	239.2	11.2	49.6	4.43

According to Table 5, increasing both the concrete compressive strength and the steel section yield stress leads to an increase in frame strength. However, for frames with steel beams, the yield stress of the steel section has a more pronounced influence on the overall strength compared to concrete compressive strength. Moreover, the effect of increasing the steel yield stress is greater in frames with a concrete compressive strength of 30 MPa than in those with a compressive strength of 70 MPa.

Table 5. *Results of FEA of frame with steel beam*

Sample	Py (kN)	Δy (mm)	Δu (mm)	μ
Frame 5	116.4	7	37.82	5.4
Frame 6	170	7.25	31.8	3.98
Frame 7	176.13	12.2	42	3.36
Frame 8	216.06	11.2	41.3	3.59

According to Table 6, increasing both the concrete compressive strength and the steel section yield stress results in an increase in frame strength. For frames with reinforced concrete beams, these two parameters have nearly identical effects on enhancing the overall capacity. Moreover, the influence of increasing concrete compressive strength and steel yield stress is more pronounced in frames with a concrete strength of 30 MPa compared to those with a strength of 70 MPa.

Table 6*. Result of FEA of frame with reinforced concrete beam.*

Sample	Py (kN)	Δy (mm)	Δu (mm)	μ
Frame 9	121.36	6.7	32.6	4.86
Frame 10	178.32	7.3	28.8	3.94
Frame 11	173.65	12.1	41.5	3.43
Frame 12	219.79	10	37.3	3.73

4. Conclusion

In the frame configuration consisting of both an SRC column and an SRC beam, the increase in concrete compressive strength exhibits a more dominant influence on the enhancement of frame strength compared to the increase in steel yield stress. Specifically, when the concrete compressive strength is increased from 30 MPa to 70 MPa, while the steel yield stress remains at 240 MPa, the overall frame strength improves by approximately 54.8%, indicating a substantial sensitivity of SRC systems to concrete strength. For the frame incorporating an SRC column and a steel beam, the behavior differs. In this configuration, the steel section yield stress plays the

primary role in improving the frame strength. Increasing the steel yield stress from 240 MPa to 690 MPa, while maintaining the concrete compressive strength at 30 MPa, results in a 46% increase in frame strength. This demonstrates that frames with steel beams rely more heavily on the mechanical properties of steel than on concrete strength enhancement.

In the frame composed of an SRC column and a reinforced concrete beam, both the concrete compressive strength and the steel yield stress contribute almost equally to the structural capacity. Increasing the concrete strength from 30 MPa to 70 MPa leads to a 46.93% increase in frame strength, while raising the steel yield stress from 240 MPa to 690 MPa results in a 43.1% improvement. These results indicate a balanced interaction between concrete and steel contributions in composite frames with reinforced concrete beams. Across all three frame types, the specimens with an initial concrete compressive strength of 30 MPa exhibit nearly identical yield strengths, reflecting similar elastic stiffness characteristics prior to yielding. However, when the compressive strength is increased to 70 MPa, the frame with the SRC beam demonstrates superior performance compared to the steel-beam and RC-beam configurations. This highlights the beneficial synergy between SRC columns and SRC beams under higher-strength concrete conditions, leading to.

References

Han, L.-H., Huang, H., Tao, Z. (2020). Performance of concrete-encased steel composite columns: A state-of-the-art review. Engineering Structures.

Tao, Z., Wang, Z., Han, L.-H. (2018). Analytical models for confined concrete in composite members. Journal of Structural Engineering.

Uy, B., Patel, V., Liew, J.Y.R. (2011). Behavior of composite columns in fire and ambient conditions. Journal of Constructional Steel Research.

Zheng, Y., Li, Y., & Xu, L. (2017). Cyclic performance of SRC composite columns under high axial load. Engineering Structures.

Li, Z., Chen, S., & Sun, W. (2019). Nonlinear FE simulation of SRC beam-column joints using ABAQUS. Composite Structures.

Hossain, T., Ahmed, M. (2021). Finite element modeling of composite columns subjected to monotonic loading. Structures.

Wang, J., Xu, Q., & Luo, X. (2021). Effects of concrete strength on the seismic behavior of composite columns. Structural Engineering and Mechanics.

Zhang, H., Zhou, X., & Feng, D. (2022). Influence of steel yield strength on the nonlinear response of composite columns. Thin-Walled Structures.

Chen, C. C., & Lin, N. J. (2006). *Analytical model for predicting axial capacity and behavior of concrete-encased steel composite stub columns*. Journal of Constructional Steel Research, 62(5), 423–434.

Mirza, S. A. (1989). *Parametric study of composite column strength variability*. Journal of Constructional Steel Research, 14(2), 121–137.

Mirza, S. A., & Skrabek, B. W. (1992). *Statistical analysis of slender composite beam-column strength*. Journal of Structural Engineering, 118(5), 1312–1332.

Lee, J., & Fenves, G. (2021). Advances in concrete damaged plasticity modeling for nonlinear structural analysis. Engineering Structures, 243, 112–145.

Niu, D., Song, Z., & Wu, Y. (2020). Enhanced stress–strain model for confined concrete incorporating modern confinement effects. Construction and Building Materials, 256, 119–136.

Tao, Z., Han, L.-H., & Wang, Z. (2018). Behaviour of confined and unconfined concrete in composite columns. Journal of Structural Engineering, 144(6).

Yu, T., & Teng, J. G. (2019). Stress–strain behavior of FRP- and steel-confined concrete: Unified models and comparisons. Composite Structures, 226, 111–123.

Zhang, H., Zhou, X., & Feng, D. (2022). Revisiting constitutive models for confined concrete with updated experimental data. Thin-Walled Structures, 176, 109–212.